

Chiral symmetry restoration in strange hadronic matter

P. Wang, V. E. Lyubovitskij, Th. Gutsche, and Amand Faessler
*Institut für Theoretische Physik, Universität Tübingen, Auf der Morgenstelle 14,
D-72076 Tübingen, Germany*

Abstract

The phase transition of chiral symmetry restoration in strange hadronic matter is studied in the chiral SU(3) quark mean field model. When the baryon density is larger than a critical density ρ_c , the minimal energy density of the system occurs at the point where the effective masses of nucleon, Λ or Ξ drop to zero. The physical quantities change discontinuously at this density and the system will be in the phase of chiral symmetry restoration. A rich phase structure of strange hadronic matter with different strangeness fraction f_s is obtained.

PACS number(s): 21.65.+f; 12.39.-x; 11.30.Rd

Keywords: chiral symmetry, quark mean field, strange matter, phase transition

I. INTRODUCTION

It is generally believed that there are two phase transitions in hot and dense hadronic matter [1,2]. One is deconfinement which is related to the transition from hadronic to quark matter and the other is the chiral symmetry restoration. Above the critical temperature T_c , the hadronic states may survive in the high temperature phase of QCD [17]. In general, deconfinement has been described in terms of Polyakov loop. Lattice QCD simulations show that chiral symmetry restoration and deconfinement occur at the same critical temperature T_c [3]. The qualitative feature that at high temperature deconfinement and chiral symmetry restoration come together is not much of a mystery: in the deconfinement phase quarks are hypothetically free and their masses tend to zero. It is a longstanding puzzle however why deconfinement and chiral symmetry restoration occur quantitatively at the same temperature, though there are some explanations to connect these two phase transitions [4].

Some of the signals related to the appearance of the deconfined phase are the phenomenon of strangeness enhancement and the J/Ψ suppression [5,6]. A direct signature of the formation of the deconfined phase is the existence of strangelets. Many ultrarelativistic heavy-ion collision experiments at Brookhaven and CERN are proposed to search for (meta)stable lumps of such kind of strangelets. Up to now, there is no experiment which confirms the existence of strangelets. Ardouin et al. [7] presented a novel method which can be applied to characterize the possible existence of a strange quark matter distillation process in heavy-ion collisions. Asakawa et al. [8] pointed out that the size of the average

fluctuations of net baryon number and electric charge in a finite volume of hadronic matter differs widely between the confined and deconfined phases which in turn can be exploited as indicators for the formation of a quark-gluon plasma in relativistic heavy-ion collisions. The E864 collaboration found that there was no evidence for neutral strangelet production in 11.5 GeV/c per nucleon Au+Pb collisions [9]. The new measurement of NA50 revealed a steady significant decrease in the J/Ψ production rate up to the most central Pb-Pb collisions and it clearly rules out the presently available conventional (hadronic) models of J/Ψ suppression. This new observation leads to a natural explanation in the framework of the formation of a deconfined state of quarks and gluons [10].

In the context of the present work we investigate whether chiral symmetry restoration occurs only when quarks are deconfined, i.e., whether the phase transition of chiral symmetry restoration can appear in hadronic matter. In Ref. [11], it was pointed out that chiral symmetry breaking will strengthen in nuclear matter. Furthermore, the quark condensate will increase with baryon density for values higher than about $0.7\rho_0$, where ρ_0 is the saturation density of nuclear matter. The quark condensate in the nuclear medium has also been evaluated in the framework of mean-field theory, the Nambu-Jona-Lasinio model, the relativistic Brueckner Hartree-Fock approach, and the bare vertex nuclear Schwinger-Dyson formalism [12]- [15]. The results of these models indicate that the quark condensate in nuclear matter is considerably reduced already for saturation density. The effect of chiral symmetry restoration can also be connected to the effective baryon mass [16]. At the critical temperature T_c , the hadronic states may survive in the high temperature phase of QCD [17] where the mesons are massless in the chiral limit. Due to the Brown-Rho scaling [16], the baryon mass will also be zero at this time. In general, deconfinement has been described in terms of Polyakov loop. Mocsy *et al.* [18] illustrated that the deconfinement is a consequence of chiral symmetry restoration in the presence of massless quarks in the fundamental representation. On the other hand, Brown *et al.* [19] show that chiral symmetry restoration is accompanied by the vanishing of the trace anomaly which is connected with the baryon mass. Therefore, the baryon mass can be used as an order parameter for chiral symmetry restoration.

Presently, the complex action of QCD at finite chemical potential makes it difficult to study finite-density QCD properties directly from first principle lattice calculations. We therefore have to resort even more to phenomenological models to investigate hadronic matter. The symmetries of QCD can be used as a guideline to determine largely how the hadrons should interact with each other. Following this idea, models based on $SU(2)_L \times SU(2)_R$ symmetry and scale invariance were proposed. These effective models have been widely used in the last years to investigate nuclear matter and finite nuclei both at zero and at finite temperature [20]- [26]. Papazoglou *et al.* extended the effective chiral models to $SU(3)_L \times SU(3)_R$ including the full baryon octet [27,28]. Although these chiral models indicate that the effective nucleon mass decreases with density, there is no phase transition with respect to chiral symmetry restoration. As an extension we proposed the chiral $SU(3)$ quark mean field model and investigated hadronic and quark matter [29]- [31]. The chiral symmetry restoration of nuclear matter was also studied in this model and a phase transition was found [32]. At some critical baryon density, the effective nucleon mass and the quark condensate decrease discontinuously. In the present work we will extend the investigation to study chiral symmetry restoration of strange hadronic matter which includes Λ , Σ and Ξ

hyperons.

The paper is organized as follows. The basic features of the model are introduced in Sec. II. In Sec. III, we use this model to investigate chiral symmetry restoration of strange hadronic matter. In Sec. IV we present the numerical results. In Sec. V we summarize our conclusions.

II. THE MODEL

Our considerations are based on the chiral SU(3) quark mean field model (for details see Refs. [29]- [30]), which contains quarks and mesons as basic degrees of freedom. Quarks are confined into baryons by an effective potential. The quark meson interaction and meson self-interaction are based on the SU(3) chiral symmetry. Through the mechanism of spontaneous chiral symmetry breaking, the resulting constituent quarks and mesons (except for the pseudoscalar ones) obtain masses. The introduction of an explicit symmetry breaking term in the meson self-interaction generates the masses of the pseudoscalar mesons which satisfy the PCAC relation. The explicit symmetry breaking term of the quark meson interaction leads in turn to reasonable hyperon potentials in hadronic matter. For completeness, we introduce the main concepts of the model in this section.

In the chiral limit, the quark field q can be split into left and right-handed parts q_L and q_R : $q = q_L + q_R$. Under SU(3)_L × SU(3)_R they transform as

$$q_L \rightarrow q'_L = L q_L, \quad q_R \rightarrow q'_R = R q_R. \quad (1)$$

The spin-0 mesons are written in the compact form

$$M(M^+) = \Sigma \pm i\Pi = \frac{1}{\sqrt{2}} \sum_{a=0}^8 (s^a \pm ip^a) \lambda^a, \quad (2)$$

where s^a and p^a are the nonets of scalar and pseudoscalar mesons, respectively, λ^a ($a = 1, \dots, 8$) are the Gell-Mann matrices, and $\lambda^0 = \sqrt{\frac{2}{3}} I$. The alternatives, plus and minus signs correspond to M and M^+ . Under chiral SU(3) transformations, M and M^+ transform as $M \rightarrow M' = LMR^+$ and $M^+ \rightarrow M'^+ = RM^+L^+$. As for the spin-0 mesons, the spin-1 mesons are set up in a similar way as

$$l_\mu(r_\mu) = \frac{1}{2} (V_\mu \pm A_\mu) = \frac{1}{2\sqrt{2}} \sum_{a=0}^8 (v_\mu^a \pm a_\mu^a) \lambda^a \quad (3)$$

with the transformation properties: $l_\mu \rightarrow l'_\mu = Ll_\mu L^+$, $r_\mu \rightarrow r'_\mu = Rr_\mu R^+$. The matrices Σ , Π , V_μ and A_μ can be written in a form where the physical states are explicit. For the scalar and vector nonets, we have the expressions

$$\Sigma = \frac{1}{\sqrt{2}} \sum_{a=0}^8 s^a \lambda^a = \begin{pmatrix} \frac{1}{\sqrt{2}} (\sigma + a_0^0) & a_0^+ & K^{*+} \\ a_0^- & \frac{1}{\sqrt{2}} (\sigma - a_0^0) & K^{*0} \\ K^{*-} & \bar{K}^{*0} & \zeta \end{pmatrix}, \quad (4)$$

$$V_\mu = \frac{1}{\sqrt{2}} \sum_{a=0}^8 v_\mu^a \lambda^a = \begin{pmatrix} \frac{1}{\sqrt{2}} (\omega_\mu + \rho_\mu^0) & \rho_\mu^+ & K_\mu^{*+} \\ \rho_\mu^- & \frac{1}{\sqrt{2}} (\omega_\mu - \rho_\mu^0) & K_\mu^{*0} \\ K_\mu^{*-} & \bar{K}_\mu^{*0} & \phi_\mu \end{pmatrix}. \quad (5)$$

Pseudoscalar and pseudovector nonet mesons can be written in a similar fashion.

The total effective Lagrangian is set up as

$$\mathcal{L}_{\text{eff}} = \mathcal{L}_{q0} + \mathcal{L}_{qM} + \mathcal{L}_{\Sigma\Sigma} + \mathcal{L}_{VV} + \mathcal{L}_{\chi SB} + \mathcal{L}_{\Delta m_s} + \mathcal{L}_h + \mathcal{L}_c, \quad (6)$$

where $\mathcal{L}_{q0} = \bar{q} i \gamma^\mu \partial_\mu q$ is the free part for massless quarks. The quark-meson interaction \mathcal{L}_{qM} can be written in a chiral SU(3) invariant way as

$$\begin{aligned} \mathcal{L}_{qM} &= g_s \left(\bar{\Psi}_L M \Psi_R + \bar{\Psi}_R M^+ \Psi_L \right) - g_v \left(\bar{\Psi}_L \gamma^\mu l_\mu \Psi_L + \bar{\Psi}_R \gamma^\mu r_\mu \Psi_R \right) \\ &= \frac{g_s}{\sqrt{2}} \bar{\Psi} \left(\sum_{a=0}^8 s_a \lambda_a + i \gamma^5 \sum_{a=0}^8 p_a \lambda_a \right) \Psi - \frac{g_v}{2\sqrt{2}} \bar{\Psi} \left(\gamma^\mu \sum_{a=0}^8 v_\mu^a \lambda_a - \gamma^\mu \gamma^5 \sum_{a=0}^8 a_\mu^a \lambda_a \right) \Psi. \end{aligned} \quad (7)$$

The chiral invariant quark-meson interaction can be traced back to the Georgi-Manohar model [33] where the chiral symmetry is realized in nonlinear way with pseudoscalar mesons. In our model, we include both the scalar and vector mesons which are important in describing hadronic matter. The constituent quark masses are obtained through the spontaneous breaking of symmetry and they are not added by hand as in the Georgi-Manohar model. In the mean field approximation, the chiral-invariant scalar meson $\mathcal{L}_{\Sigma\Sigma}$ and vector meson \mathcal{L}_{VV} self-interaction terms are written as [29]- [30]

$$\begin{aligned} \mathcal{L}_{\Sigma\Sigma} &= -\frac{1}{2} k_0 \chi^2 (\sigma^2 + \zeta^2) + k_1 (\sigma^2 + \zeta^2)^2 + k_2 \left(\frac{\sigma^4}{2} + \zeta^4 \right) + k_3 \chi \sigma^2 \zeta \\ &\quad - k_4 \chi^4 - \frac{1}{4} \chi^4 \ln \frac{\chi^4}{\chi_0^4} + \frac{\delta}{3} \chi^4 \ln \frac{\sigma^2 \zeta}{\sigma_0^2 \zeta_0}, \end{aligned} \quad (8)$$

$$\mathcal{L}_{VV} = \frac{1}{2} \frac{\chi^2}{\chi_0^2} \left(m_\omega^2 \omega^2 + m_\rho^2 \rho^2 + m_\phi^2 \phi^2 \right) + g_4 \left(\omega^4 + 6\omega^2 \rho^2 + \rho^4 + 2\phi^4 \right), \quad (9)$$

where $\delta = 6/33$; σ_0 , ζ_0 and χ_0 are the vacuum expectation values [31] of the corresponding mean fields σ , ζ and χ .

Chiral symmetry requires the following basic relations for the quark-meson coupling constants:

$$\frac{g_s}{\sqrt{2}} = g_{a0}^u = -g_{a0}^d = g_\sigma^u = g_\sigma^d = \dots = \frac{1}{\sqrt{2}} g_\zeta^s, \quad g_{a0}^s = g_\sigma^s = g_\zeta^u = g_\zeta^d = 0, \quad (10)$$

$$\frac{g_v}{2\sqrt{2}} = g_{\rho^0}^u = -g_{\rho^0}^d = g_\omega^u = g_\omega^d = \dots = \frac{1}{\sqrt{2}} g_\phi^s, \quad g_\omega^s = g_{\rho^0}^s = g_\phi^u = g_\phi^d = 0. \quad (11)$$

Note, the values of σ_0 , ζ_0 and χ_0 are determined from a minimization of the thermodynamical potential [31] (see below the procedure for σ_0 and ζ_0 in Eqs. (34) and (35)). On the other hand, the parameters σ_0 and ζ_0 are constrained by the spontaneous breaking of chiral symmetry and are expressed by the pion ($F_\pi = 93$ MeV) and the kaon ($F_K = 115$ MeV) leptonic decay constants as:

$$\sigma_0 = -F_\pi \quad \zeta_0 = \frac{1}{\sqrt{2}}(F_\pi - 2F_K) \quad (12)$$

Masses of vector mesons derived in Eq. (9) are density dependent and are expressed as

$$m_\omega^2 = m_\rho^2 = \frac{m_v^2}{1 - \frac{1}{2}\mu\sigma_0^2}, \quad \text{and} \quad m_\phi^2 = \frac{m_v^2}{1 - \mu\zeta_0^2}, \quad (13)$$

where the vacuum value of the vector meson mass $m_v = 673.6$ MeV and the density parameter $\mu = 2.34$ fm² are chosen to reproduce $m_\omega = 783$ MeV and $m_\phi = 1020$ MeV.

The Lagrangian $\mathcal{L}_{\chi SB}$ generates the nonvanishing masses of pseudoscalar mesons

$$\mathcal{L}_{\chi SB} = \frac{\chi^2}{\chi_0^2} \left[m_\pi^2 F_\pi \sigma + \left(\sqrt{2} m_K^2 F_K - \frac{m_\pi^2}{\sqrt{2}} F_\pi \right) \zeta \right], \quad (14)$$

leading to a nonvanishing divergence of the axial currents which in turn satisfy the partial conserved axial-vector current (PCAC) relations for π and K mesons. Pseudoscalar, scalar mesons and also the dilaton field χ obtain mass terms by spontaneous breaking of chiral symmetry in the Lagrangian (8). The masses of u , d and s quarks are generated by the vacuum expectation values of the two scalar mesons σ and ζ . To obtain the correct constituent mass of the strange quark, an additional mass term has to be added:

$$\mathcal{L}_{\Delta m_s} = -\Delta m_s \bar{q} S q \quad (15)$$

where $S = \frac{1}{3} (I - \lambda_8 \sqrt{3}) = \text{diag}(0, 0, 1)$ is the strangeness quark matrix. Based on above mechanisms, the quark constituent masses are finally given by

$$m_u = m_d = -\frac{g_s}{\sqrt{2}} \sigma_0 \quad \text{and} \quad m_s = -g_s \zeta_0 + \Delta m_s. \quad (16)$$

The parameters $g_s = 4.76$ and $\Delta m_s = 29$ MeV are determined from $m_q = 313$ MeV and $m_s = 490$ MeV. In order to obtain reasonable hyperon potentials in hadronic matter we include an additional coupling between strange quarks and the scalar mesons σ and ζ [29]. This term is expressed as

$$\mathcal{L}_h = (h_1 \sigma + h_2 \zeta) \bar{s} s. \quad (17)$$

In the quark mean field model, quarks are confined in baryons by the Lagrangian $\mathcal{L}_c = -\bar{\Psi} \chi_c \Psi$. The Dirac equation for a quark field Ψ_{ij} under the additional influence of the meson mean fields is given by

$$\left[-i\vec{\alpha} \cdot \vec{\nabla} + \chi_c(r) + \beta m_i^* \right] \Psi_{ij} = e_i^* \Psi_{ij}, \quad (18)$$

where $\vec{\alpha} = \gamma^0 \vec{\gamma}$, $\beta = \gamma^0$, the subscripts i and j denote the quark i ($i = u, d, s$) in a baryon of type j ($j = N, \Lambda, \Sigma, \Xi$); $\chi_c(r)$ is a confinement potential, i.e. a static potential providing confinement of quarks by meson mean-field configurations.

The quark mass m_i^* and energy e_i^* are defined as

$$m_i^* = -g_\sigma^i \sigma - g_\zeta^i \zeta + m_{i0} \quad (19)$$

and

$$e_i^* = e_i - g_\omega^i \omega - g_\phi^i \phi, \quad (20)$$

where e_i is the energy of the quark under the influence of the meson mean fields. Here $m_{i0} = 0$ for $i = u, d$ (nonstrange quark) and $m_{i0} = \Delta m_s = 29$ MeV for $i = s$ (strange quark).

The confining potential χ_c is chosen as a combination of scalar (S) and scalar-vector (SV) potentials as in Ref. [30,32]:

$$\chi_c(r) = \frac{1}{2}[\chi_c^S(r) + \chi_c^{SV}(r)] \quad (21)$$

with

$$\chi_c^S(r) = \frac{1}{4}k_c r^2, \quad (22)$$

and

$$\chi_c^{SV}(r) = \frac{1}{4}k_c r^2(1 + \gamma^0). \quad (23)$$

The coupling k_c is taken as $k_c = 1$ ($\text{GeV} \times \text{fm}^{-2}$) to get baryon radii of about 0.6 fm. Using the solution of the Dirac equation (18) for the quark energy e_i^* we can define the effective mass of the baryon j as

$$M_j^* = \sqrt{E_j^{*2} - \langle p_{j\,cm}^{*2} \rangle}, \quad (24)$$

where $E_j^* = \sum_i n_{ij} e_i^* + E_{j\,spin}$ is the baryon energy and $\langle p_{j\,cm}^{*2} \rangle$ is the subtraction of the spurious center of mass motion. In the expression for the baryon energy n_{ij} is the number of quarks with flavor "i" in a baryon with flavor j with $j = N \{p, n\}, \Sigma \{\Sigma^\pm, \Sigma^0\}, \Xi \{\Xi^0, \Xi^-\}, \Lambda$ and $E_{j\,spin}$ is the correction to the baryon energy due to the spin-spin quark interactions. We determine the values of $E_{j\,spin}$ as

$$E_{N\,spin} = -770.3 \text{ MeV}, \quad E_{\Lambda\,spin} = -756.9 \text{ MeV}, \quad (25)$$

$$E_{\Sigma\,spin} = -690.9 \text{ MeV}, \quad E_{\Xi\,spin} = -717.6 \text{ MeV}$$

from a fit to the data for baryon masses: $M_N = 939$ MeV, $M_\Lambda = 1116$ MeV, $M_\Sigma = 1196$ MeV and $M_\Xi = 1318$ MeV. For illustration we also present the vacuum values of quark energies and of the center of mass corrections:

$$e_u = e_d = 663.0 \text{ MeV}, \quad e_s = 799.2 \text{ MeV}, \quad (26)$$

$$\langle p_{N\,cm}^2 \rangle = 15.5 \text{ fm}^{-2}, \quad \langle p_{\Lambda\,cm}^2 \rangle = \langle p_{\Sigma\,cm}^2 \rangle = 16.1 \text{ fm}^{-2}, \quad \langle p_{\Xi\,cm}^2 \rangle = 16.6 \text{ fm}^{-2}.$$

III. STRANGE HADRONIC MATTER

Based on the previously defined quark mean field model the effective Lagrangian for study of strange hadronic systems is written as

$$\begin{aligned} \mathcal{L} = & \sum_{B=N,\Lambda,\Sigma,\Xi} \bar{\psi}_B \gamma^\mu (i \partial_\mu - M_B^* - g_\omega^B \omega_\mu - g_\phi^B \phi_\mu) \psi_B \\ & + \frac{1}{2} \partial_\mu \sigma \partial^\mu \sigma + \frac{1}{2} \partial_\mu \zeta \partial^\mu \zeta + \frac{1}{2} \partial_\mu \chi \partial^\mu \chi - \frac{1}{4} F_{\mu\nu} F^{\mu\nu} - \frac{1}{4} S_{\mu\nu} S^{\mu\nu} + \mathcal{L}_M, \end{aligned} \quad (27)$$

where

$$F_{\mu\nu} = \partial_\mu \omega_\nu - \partial_\nu \omega_\mu \quad \text{and} \quad S_{\mu\nu} = \partial_\mu \phi_\nu - \partial_\nu \phi_\mu \quad (28)$$

are the conventional vector meson field (ω and ϕ) strength tensors.

The term

$$\mathcal{L}_M = \mathcal{L}_{\Sigma\Sigma} + \mathcal{L}_{VV} + \mathcal{L}_{\chi SB} \quad (29)$$

describes the interaction between mesons which includes the scalar meson self-interaction $\mathcal{L}_{\Sigma\Sigma}$, the vector meson self-interaction \mathcal{L}_{VV} and the explicit chiral symmetry breaking term $\mathcal{L}_{\chi SB}$ defined previously in Eqs. (8), (9) and (14). The Lagrangian \mathcal{L}_M involves scalar (σ , ζ and χ) and vector (ω and ϕ) mesons. The interactions between quarks and scalar mesons result in the effective baryon masses M_B^* , where subscript B labels the baryon flavor $B = N, \Lambda, \Sigma$ or Ξ . The interactions between quarks and vector mesons generate the baryon-vector meson interaction terms of Eq. (27). The corresponding vector coupling constants g_ω^B and g_ϕ^B satisfy the SU(3) flavor symmetry relations:

$$g_\omega^\Lambda = g_\omega^\Sigma = 2g_\omega^\Xi = \frac{2}{3}g_\omega^N = 2g_\omega^u = \frac{g_v}{\sqrt{2}} \quad \text{and} \quad g_\phi^\Lambda = g_\phi^\Sigma = \frac{1}{2}g_\phi^\Xi = \frac{\sqrt{2}}{3}g_\omega^N = g_\phi^s = \frac{g_v}{2}. \quad (30)$$

At finite temperature and density, the thermodynamical potential is defined as

$$\begin{aligned} \Omega = & - \sum_{B=N,\Lambda,\Sigma,\Xi} \frac{g_B k_B T}{(2\pi)^3} \int_0^\infty d^3k \left\{ \ln \left(1 + e^{-[E_B^*(k) - \nu_B]/k_B T} \right) \right. \\ & \left. + \ln \left(1 + e^{-[E_B^*(k) + \nu_B]/k_B T} \right) \right\} - \mathcal{L}_M, \end{aligned} \quad (31)$$

where $E_B^*(k) = \sqrt{M_B^{*2} + k^2}$ and g_B is the degeneracy of baryon B ($g_{N,\Xi} = 2$, $g_\Lambda = 1$ and $g_\Sigma = 3$). The quantity ν_B is related to the usual chemical potential μ_B by

$$\nu_B = \mu_B - g_\omega^B \omega - g_\phi^B \phi. \quad (32)$$

At zero temperature, the thermodynamical potential of symmetric hadronic matter can be expressed as

$$\begin{aligned} \Omega = & \sum_{B=N,\Lambda,\Sigma,\Xi} \frac{g_B}{12\pi^2} \left\{ \nu_B [\nu_B^2 - M_B^{*2}]^{1/2} [2\nu_B^2 - 5M_B^{*2}] \right. \\ & \left. + 3M_B^{*4} \ln \left[\frac{\nu_B + (\nu_B^2 - M_B^{*2})^{1/2}}{M_B^*} \right] \right\} - \mathcal{L}_M. \end{aligned} \quad (33)$$

The energy per volume and the pressure of the system can be derived as $\varepsilon = \Omega + \nu_B \rho_B$ and $p = -\Omega$, respectively, where ρ_B is the baryon density.

The mean field equations for the mesons ϕ_i are obtained with $\frac{\partial \Omega}{\partial \phi_i} = 0$. For example, the equations for the scalar mesons σ , ζ are expressed as

$$k_0 \chi^2 \sigma - 4k_1 (\sigma^2 + \zeta^2) \sigma - 2k_2 \sigma^3 - 2k_3 \chi \sigma \zeta - \frac{2\delta}{3\sigma} \chi^4 + \frac{\chi^2}{\chi_0^2} m_\pi^2 F_\pi - \left(\frac{\chi}{\chi_0} \right)^2 m_\omega \omega^2 \frac{\partial m_\omega}{\partial \sigma} + \sum_{B=N,\Lambda,\Sigma,\Xi} \frac{\partial M_B^*}{\partial \sigma} \langle \bar{\psi}_B \psi_B \rangle = 0, \quad (34)$$

$$k_0 \chi^2 \zeta - 4k_1 (\sigma^2 + \zeta^2) \zeta - 4k_2 \zeta^3 - k_3 \chi \sigma^2 - \frac{\delta}{3\zeta} \chi^4 + \frac{\chi^2}{\chi_0^2} \left(\sqrt{2} m_k^2 F_k - \frac{1}{\sqrt{2}} m_\pi^2 F_\pi \right) - \left(\frac{\chi}{\chi_0} \right)^2 m_\phi \phi^2 \frac{\partial m_\phi}{\partial \zeta} + \sum_{B=\Lambda,\Sigma,\Xi} \frac{\partial M_B^*}{\partial \zeta} \langle \bar{\psi}_B \psi_B \rangle = 0, \quad (35)$$

where

$$\begin{aligned} \langle \bar{\psi}_B \psi_B \rangle &= \frac{g_B M_B^*}{\pi^2} \int_0^{k_{FB}} dk \frac{k^2}{\sqrt{M_B^{*2} + k^2}} \\ &= \frac{g_B M_B^{*3}}{2\pi^2} \left[\frac{k_{FB}}{M_B^*} \sqrt{1 + \frac{k_{FB}^2}{M_B^{*2}}} - \ln \left(\frac{k_{FB}}{M_B^*} + \sqrt{1 + \frac{k_{FB}^2}{M_B^{*2}}} \right) \right] \end{aligned} \quad (36)$$

is the baryon condensate and $k_{FB} = \sqrt{\nu_B^2 - M_B^{*2}}$ is the Fermi momentum. At zero baryon density, the vacuum expectation values of σ and ζ have been introduced in Eq. (12). With an increase of the baryon density the values of σ and ζ rise which in turn result in a decrease of the effective baryon masses. The effective baryon mass M_B^* are generally in the region

$$0 \leq M_B^*(\sigma, \zeta) \leq M_B^*(\sigma_0, \zeta_0). \quad (37)$$

The ranges of mean field values for σ and ζ

$$\sigma_0 \leq \sigma \leq \sigma_b, \quad \zeta_0 \leq \zeta \leq \zeta_b, \quad (38)$$

where the upper values σ_b and ζ_b are determined by $M_N^* = 0$, $M_\Lambda^* = 0$ or $M_\Xi^* = 0$. Since the Σ hyperon has the same quark flavor content as the Λ hyperon, its effective mass is always larger than that of the Λ . At a specific point for high baryon density, the minimum of the thermodynamical potential Ω appears not inside the region, but at the boundary of values given for σ and ζ . In this limit, Eqs. (34) and (35) for σ and ζ are not valid any more. At the boundary, the mean fields σ and ζ satisfy the equations

$$\frac{\partial \Omega}{\partial Z} = 0, \quad dZ = \sqrt{d\sigma^2 + d\zeta^2}, \quad (39)$$

where Z is in the boundary and $d\sigma$, $d\zeta$ are constrained by

$$\frac{\partial M_B^*(\sigma, \zeta)}{\partial \sigma} d\sigma + \frac{\partial M_B^*(\sigma, \zeta)}{\partial \zeta} d\zeta = 0 \quad (B = N, \Lambda, \Xi). \quad (40)$$

Therefore, if the minimum of the thermodynamical potential appears for $M_B^*(\sigma, \zeta) = 0$, the equations for σ and ζ can be deduced from

$$M_B^*(\sigma, \zeta) = 0, \quad (41)$$

$$\frac{\partial \Omega}{\partial \sigma} \frac{1}{\sqrt{1 + \left(\frac{\partial M_B^*/\partial \sigma}{\partial M_B^*/\partial \zeta}\right)^2}} + \frac{\partial \Omega}{\partial \zeta} \frac{1}{\sqrt{1 + \left(\frac{\partial M_B^*/\partial \zeta}{\partial M_B^*/\partial \sigma}\right)^2}} = 0. \quad (42)$$

For the special case, when M_N^* is only a function of σ , Eq. (42) is identical to Eq. (35).

IV. NUMERICAL RESULTS

The parameters of the chiral SU(3) quark mean field model are determined, as previously done [29]- [30], by the meson masses in vacuum and by the properties of nuclear matter. The confining potential χ_c , is chosen as in Refs. [30,32], where it was shown in comparison with two other two types of potentials that it is the best choice to describe finite systems. The model parameters are summarized as follows:

$$\begin{aligned} k_0 = 4.21, \quad k_1 = 2.26, \quad k_2 = -10.16, \quad k_3 = -4.38, \quad k_4 = -0.13, \\ g_4 = 7.5, \quad h_1 = -2.07, \quad h_2 = 2.90, \quad g_s = 4.76, \quad g_v = 10.37, \quad k_c = 1 \text{ (GeV} \times \text{fm}^{-2}\text{)}. \end{aligned} \quad (43)$$

We do not mention the parameters which are fixed from experimental data or from the chiral symmetry constraints. In the previous section, we already mentioned that the values of σ and ζ are determined by minimization of the thermodynamical potential Ω . At zero temperature, the scalar meson mean field values can be obtained by minimizing the energy per volume ε . For nonstrange matter, ε can be expressed as a function of σ or of the effective nucleon mass M_N^* . At some critical baryon density the minimum of ε appears at $M_N^* = 0$, a scenario which has been studied in Ref. [32]. For strange hadronic matter ε is a function of the mean field values σ and ζ . At a given strangeness fraction, when the baryon density is low, there is a minimum of ε where the effective nucleon and hyperon masses have nonzero values. In most other models, for any values of the strangeness fraction and the baryon density, a solution for the mean field equations corresponding to (34) and (35), can be obtained, that is the minimum of ε occurs for nonzero effective baryon masses. However, in the present chiral SU(3) quark mean field model, the minimum of ε will appear on the boundary of σ and ζ at high baryon density for a fixed strangeness fraction.

In Fig. 1 we plot the boundary of σ and ζ resulting from the model. The solid, dashed and dotted lines correspond to the three boundaries where the effective baryon masses are zero, i.e., $M_N^* = 0$, $M_\Lambda^* = 0$ and $M_\Xi^* = 0$. The two coordinate axis and the three boundaries form an area ABCDE. Inside this area, the effective baryon masses are nonzero. On the boundary the dynamical equations (34) and (35) for σ and ζ have to be replaced by equations (41) and (42). The numerical calculations show that for small strangeness fraction and at

sufficiently high baryon density the minimum of ε corresponds to the case of the solid line with a vanishing effective nucleon mass. For large strangeness fraction, the minimum of ε will coincide with the dotted line defined by a zero effective mass of the Ξ hyperon. The minimum of ε will never correspond to case of the dashed line (except at the points B and C) where only M_Λ^* vanishes. At the point B both M_N^* and M_Λ^* are zero, whereas point C is set by vanishing values of M_Λ^* and M_Ξ^* .

We next discuss the change of the effective baryon masses in dependence on the baryon density. In Fig. 2, we plot the effective baryon masses versus density at a strangeness fraction of $f_s = 0.8$. As in most other models, the effective baryon masses decrease with increasing baryon density. At this value for the strangeness fraction, the effective mass of the nucleon decreases faster than those of the other baryons. On the contrary, the effective Ξ mass decreases slower. This is because when the strangeness is small, the interaction between non-strange quarks and the σ meson is considerably stronger than the one between strange quarks and ζ . When the baryon density ρ_B reaches a value of 0.46 fm^{-3} , the effective nucleon mass drops from 0.2 GeV to zero. All other effective baryon masses also decrease discontinuously, but in these cases to finite values. In the range of $0.46 \text{ fm}^{-3} < \rho_B < 0.69 \text{ fm}^{-3}$ the effective hyperon masses continue to decrease. When the density is larger than 0.69 fm^{-3} , both nucleon and Λ masses equal zero while the Σ and Ξ masses remain at a constant and finite value.

The density dependence of the baryon masses sensitively depends on the strangeness fraction. For high strangeness fraction, the interaction between hyperons is stronger than the one between nucleons. The effective masses of hyperons with a larger strange quark content will therefore decrease faster. As a result, at a high value of the baryon density, the hyperon masses will be zero, while the nucleon mass is still finite. This effect is clearly seen from Fig. 3, where we plot the phase diagram. For the case of nonstrange hadronic matter, there are only two phases. One normal phase, where chiral symmetry is spontaneously broken, whereas at high density we have chiral symmetry restoration phase with a zero effective nucleon mass. Strange hadronic matter, corresponds to the additional presence of Λ , Σ and Ξ hyperons. Because the effective masses of the baryons drop to zero at different values of the baryon density and strangeness fraction, we obtain different chiral symmetry restoration phases. The rich phase structure is illustrated in Fig. 3 with five qualitatively different regions. Phase I refers to the normal phase with nonzero baryon masses. In the chiral symmetry restoration phase II, only the effective nucleon mass is zero. In phase III, both nucleon and Λ masses are vanishing. Phase IV, designates the case where both Λ and Ξ have zero effective masses, whereas phase V only has a vanishing value for M_Ξ^* . For different value of the strangeness fraction f_s , the normal phase I will turn into different chiral symmetry restoration phases at different critical densities. For nonstrange nuclear matter the critical baryon density is reached at a value of 0.28 fm^{-3} , where the system will be in phase II. For values of the strangeness fraction with $f_s < 1.0$, the critical density increases with growing f_s . The maximum of the critical density of about 0.5 fm^{-3} is reached for $f_s \simeq 1.0$. For the range of values $0.6 < f_s < 1.1$, when the baryon density is high enough, the chiral restoration phase can furthermore change from phase II to phase III. For larger values of the strangeness fraction, that is $f_s > 1.1$, the effective nucleon mass will not drop to zero at any density. In the range of $1.1 < f_s < 1.3$, when the density reaches a critical point, the system changes directly from phase I to phase III. At some higher density, a further

transition from phase III into phase IV takes places. For $1.3 < f_s < 1.75$, the normal phase I changes into phase IV at the critical point. For $f_s > 1.75$, chiral symmetry restoration is manifest only in phase V.

The energy per baryon E/A is defined as

$$E/A = \frac{\varepsilon}{\rho_B} - \frac{M_N \rho_N + M_\Lambda \rho_\Lambda + M_\Sigma \rho_\Sigma + M_\Xi \rho_\Xi}{\rho_B}. \quad (44)$$

In Fig. 4, we E/A in dependence on the baryon density for different strangeness fractions. For normal nuclear matter the binding energy is 16 MeV at the saturation density ρ_0 of 0.16 fm^{-3} . When the density reaches a value of about 0.28 fm^{-3} , a discontinuous decrease of energy per baryon occurs. At $\rho_B \simeq 0.31 \text{ fm}^{-3}$ there is a second minimum for E/A which is close to -16 MeV. When the density is larger than about 0.31 fm^{-3} the energy per baryon increases with growing density. As the strangeness fraction increases, the first minimum of E/A first increases and then decreases. At $f_s \simeq 1.2$, the first maximum of the binding energy is about 19 MeV. The binding energy at the second minimum is about 70 MeV and the corresponding f_s is about 1.5. The system therefore favors to have a large strangeness fraction where the corresponding density is about 3-4 times that of the saturation density ρ_0 of normal nuclear matter.

V. SUMMARY

We applied the chiral SU(3) quark mean field model to investigate the mechanism of chiral symmetry restoration in strange hadronic matter. The model is based on effective quark-meson and meson self-interactions which satisfy the chiral SU(3) symmetry constraint. Chiral symmetry restoration of nonstrange nuclear matter was studied in a previous paper [32]. When a critical baryon density is reached, the effective nucleon mass will drop to zero. This phenomenon is related to the fact that nuclear matter has its lowest energy per volume in the chiral symmetry restoration phase at high density.

In the present work we extended the discussion to strange hadronic systems including Λ , Σ and Ξ hyperons. As for the case of nonstrange nuclear matter, when the baryon density is sufficient high, the minimum of the energy per volume ε of strange matter will occur for effective baryon masses reaching a vanishing value. As it turns out, the effective masses of the different baryons do not change to zero at the same value of baryon density and strangeness fraction. In the effective model there occur four different chiral symmetry restoration phases which are characterized by zero effective masses of the different baryons. For a given strangeness fraction, when the baryon density is larger than the critical density, hadronic matter will make a transition to the corresponding chiral symmetry restoration phase with values for the critical density which is about 2-3 times larger than the nuclear saturation density ρ_0 .

The energy per baryon E/A has two minima for a given strangeness fraction. One corresponds to the normal phase, the other one occurs for the chiral symmetry restoration phase. For small strangeness fraction, that is $f_s < 1.0$, the minimum of E/A in the normal phase is lower than the one of the restored phase. For large strangeness fraction the system is favored to be in the chiral symmetry restoration phase since it occurs with a larger binding

energy. The maximal binding energy is about 70 MeV for a strangeness fraction of about 1.5.

The deconfinement phase transition may also occur at high densities. It is worthwhile to study whether the phase transition between hadronic and quark matter also takes place at values for the baryon densities which are close to the ones when chiral symmetry restoration occurs. Both the quark and the hadronic phase can be described in the chiral SU(3) quark mean field model. The model therefore opens up the possibility to also study the deconfinement phase transition, a topic which will be pursued in future studies.

Acknowledgments

P. W. would like to thank the Institute for Theoretical Physics, University of Tübingen for their hospitality. This work was supported by the Alexander von Humboldt Foundation and by the DFG under contracts FA67/25-3, GRK683.

REFERENCES

- [1] B. Müller, Nucl. Phys. A **661** (1999) 272.
- [2] U. Heinz, hep-ph/9902424.
- [3] F. Karsch, hep-lat/9903031.
- [4] C. Wetterich, Phys. Rev. D **66** (2002) 056003.
- [5] P. Koch, B. Müller, and J. Rafelski, Phys. Rep. **142** (1986) 167.
- [6] M. Gonin *et al.* [NA50 Collaboration], Nucl. Phys. A **610** (1996) 404c.
- [7] D. Ardouin *et al.*, Phys. Lett. B **446** (1999) 191.
- [8] M. Asakawa, U. W. Heinz, and B. Muller, Phys. Rev. Lett. **85** (2000) 2072.
- [9] T. A. Armstrong *et al.*, Phys. Rev. C **59** (1999) 1829.
- [10] M. C. Abreu *et al.* [NA50 Collaboration], Phys. Lett. B **477** (2000) 28.
- [11] P. J. de A. Bicudo, Phys. Rev. Lett **72** (1994) 1600.
- [12] T. D. Cohen, R. J. Furnstahl, and K. Griegel, Phys. Rev. C **45** (1992) 1881.
- [13] G. Q. Li and C. M. Ko, Phys. Lett. B **338** (1994) 118.
- [14] R. Brockmann and W. Weise, Phys. Lett. B **367** (1996) 40.
- [15] T. Mitsumori, N. Noda, H. Kouno, A. Hasegawa, and M. Nakano, Phys. Rev. C **55** (1997) 1577.
- [16] G. E. Brown and M. Rho, Phys. Rev. Lett. **66** (1991) 272.
- [17] G. E. Brown, C. H. Lee, M. Rho, and E. Shuryak, hep-ph/0312175.
- [18] A. Mocsy, F. Sannino, and K. Tuominen, hep-ph/0403160.
- [19] G. E. Brown, L. Grandchamp, C. H. Lee, and M. Rho, Phys. Rept. **391** (2004) 353.
- [20] E. K. Heide, S. Rudaz, and P. J. Ellis, Nucl. Phys. A **571** (1994) 713.
- [21] G. Carter, P. J. Ellis, and S. Rudaz, Nucl. Phys. A **603** (1996) 367; Erratum-ibid. **A608** (1996) 514.
- [22] R. J. Furnstahl, H. B. Tang, and B. D. Serot, Phys. Rev. C **52** (1995) 1368.
- [23] I. Mishustin, J. Bondorf, and M. Rho, Nucl. Phys. A **555** (1993) 215.
- [24] P. Papazoglou, J. Schaffner, S. Schramm, D. Zschesche, H. Stöcker, and W. Greiner, Phys. Rev. C **55** (1997) 1499.
- [25] L. L. Zhang, H. Q. Song, P. Wang, and R. K. Su, Phys. Rev. C **59** (1999) 3292.
- [26] P. Wang, Phys. Rev. C **61** (2000) 054904.
- [27] P. Papazoglou, S. Schramm, J. Schaffner-Bielich, H. Stöcker, and W. Greiner, Phys. Rev. C **57** (1998) 2576.
- [28] P. Papazoglou, D. Zschesche, S. Schramm, J. Schaffner-Bielich, H. Stöcker, and W. Greiner, Phys. Rev. C **59** (1999) 411.
- [29] P. Wang, Z. Y. Zhang, Y. W. Yu, R. K. Su, and H. Q. Song, Nucl. Phys. A **688** (2001) 791.
- [30] P. Wang, H. Guo, Z. Y. Zhang, Y. W. Yu, R. K. Su, and H. Q. Song, Nucl. Phys. A **705** (2002) 455.
- [31] P. Wang, V. E. Lyubovitskij, Th. Gutsche, and A. Faessler, Phys. Rev. C **67** (2003) 015210.
- [32] P. Wang, H. Guo, Y. B. Dong, Z. Y. Zhang, and Y. W. Yu, J. Phys. G **28** (2002) 2265.
- [33] A. Manohar and H. Georgi, Nucl. Phys. B **234** (1984) 189.

FIGURE CAPTIONS

Fig. 1. The boundary of σ and ζ . The solid, dashed and dotted lines are the boundaries for $M_N^* = 0$, $M_\Lambda^* = 0$ and $M_\Xi^* = 0$, respectively.

Fig. 2. The effective baryon masses versus baryon density with $f_s = 0.8$. The solid, dashed, dotted and dash-dotted lines are for nucleon, Λ , Σ and Ξ , respectively.

Fig. 3. The phase diagram for strange hadronic matter. Phase I is the normal phase. Phase II, III, IV and V are the chiral symmetry restoration phases with $M_N^* = 0$, $M_N^* = M_\Lambda^* = 0$, $M_\Lambda^* = M_\Xi^* = 0$ and $M_\Xi^* = 0$, respectively.

Fig. 4. The energy per baryon E/A versus baryon density ρ_B at different strangeness fractions.

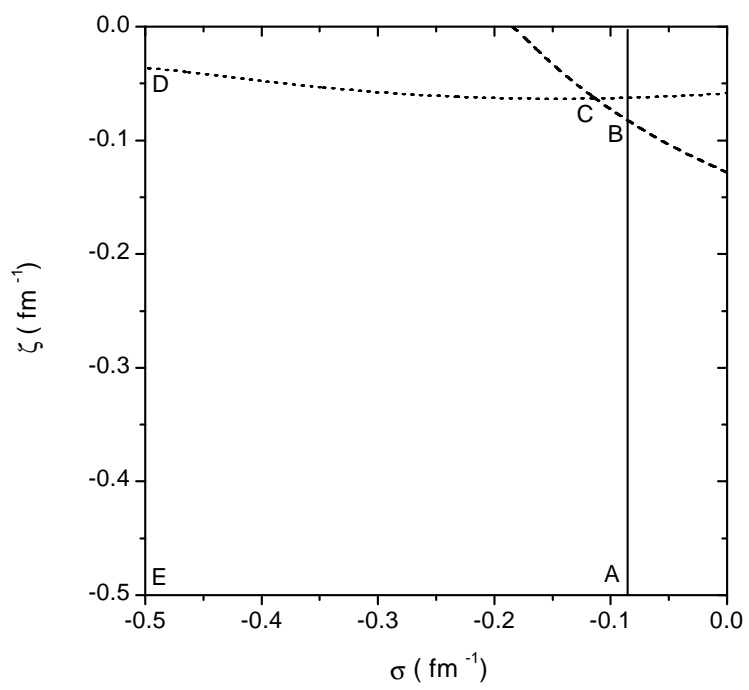


Fig. 1

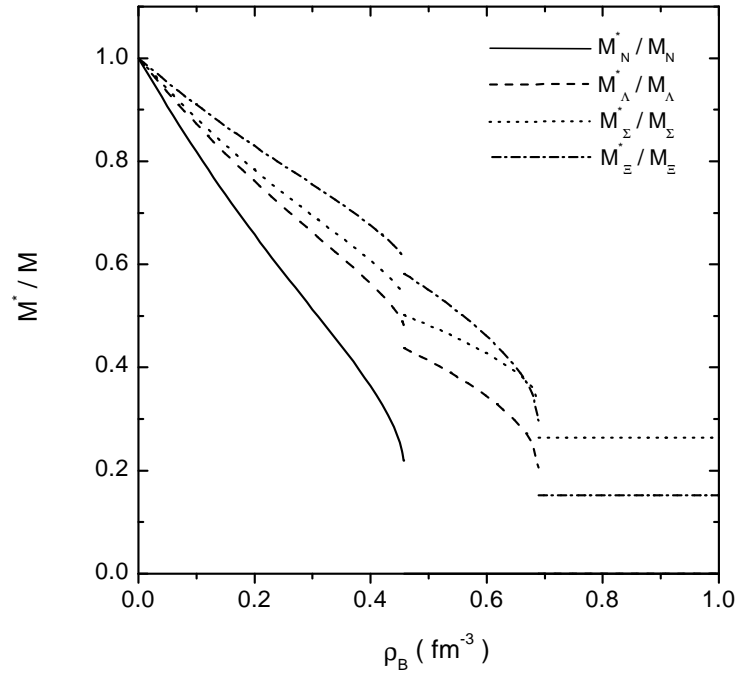


Fig. 2

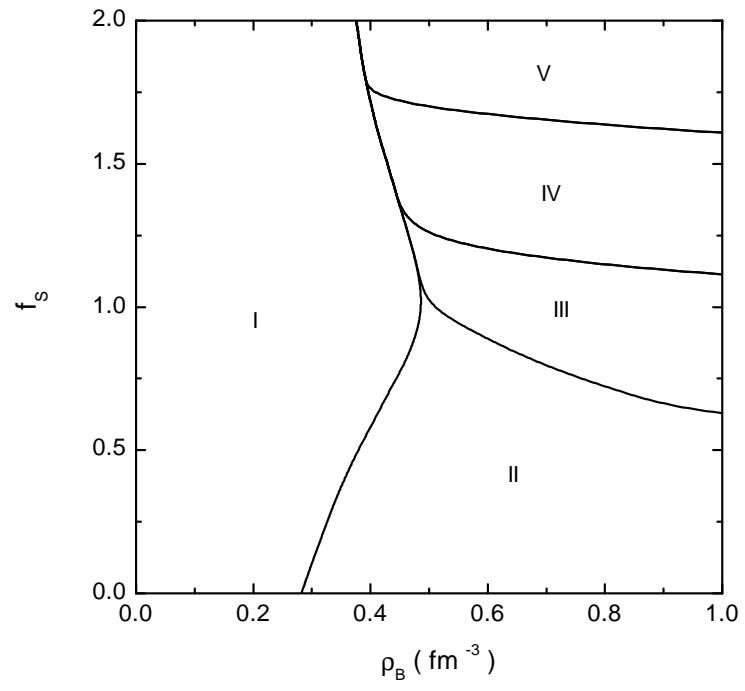


Fig. 3

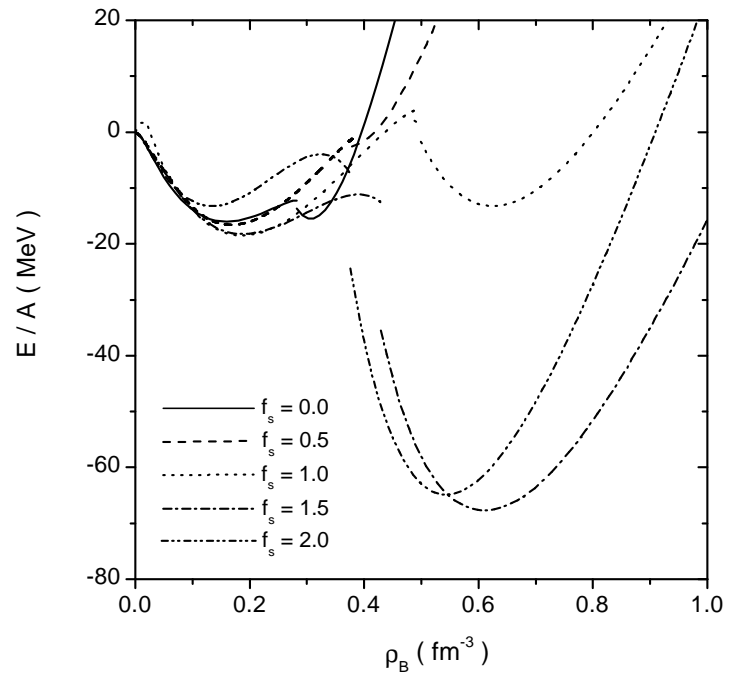


Fig. 4